Molecular Crystals and Liquid Crystals

ISSN: 1542-1406 (Print) 1563-5287 (Online) Journal homepage: http://www.tandfonline.com/loi/gmcl20

Plasmomechanics: A Colour-Changing Device Based on the Plasmonic Coupling of Gold Nanoparticles

Roberto Caputo, Ugo Cataldi, Thomas Bürgi & Cesare Umeton

To cite this article: Roberto Caputo, Ugo Cataldi, Thomas Bürgi & Cesare Umeton (2015) Plasmomechanics: A Colour-Changing Device Based on the Plasmonic Coupling of Gold Nanoparticles, Molecular Crystals and Liquid Crystals, 614:1, 20-29, DOI: 10.1080/15421406.2015.1049897

To link to this article: http://dx.doi.org/10.1080/15421406.2015.1049897

Published online: 18 Aug 2015.

Mol. Cryst. Liq. Cryst., Vol. 614: pp. 20–29, 2015

ISSN: 1542-1406 print/1563-5287 online
DOI: 10.1080/15421406.2015.1049897

Plasmomechanics: A Colour-Changing Device Based on the Plasmonic Coupling of Gold Nanoparticles

ROBERTO CAPUTO,[1,2,*] UGO CATALDI,[1,3] THOMAS BÜRGI,[3] AND CESARE UMETON[1]

[1]Department of Physics, Centre of Excellence for the Study of Innovative Functional Materials CEMIF-CAL, University of Calabria and CNR-IPCF – LICRYL, Arcavacata di Rende, Italy
[2]Laboratory of Nanotechnology, Instrumentation and Optics (LNIO), University of Technology of Troyes (UTT), Troyes Cedex, France
[3]Department of Physical Chemistry, University of Geneva, Geneva, Switzerland

We have carried out an experiment on a flexible polymeric substrate, coated with a monolayer of gold nanoparticles, which demonstrates how the combined effect of nanoparticle growth and stretching influences the average normalized gap between particles, thus modifying the extinction spectra of the sample. The study paves the way for the realization of a plasmonic strain sensor based on the plasmonic coupling of gold nanoparticles deposited onto elastomeric films: application of a mechanical stretching induces a change of colour of the device and a fine control of the applied strain allows a continuous tuning of the colour.

Introduction

Plasmonic nanoparticles show distinctive features when illuminated by light; the most known one is related to their colour, which depends on shape, size and, of course, the metal they are made of [1–3]. In addition, intriguing behaviours are exhibited when nanoparticles are very close to each other, because the resulting near-field coupling leads to intense and highly localized electric fields [4,5]. This phenomenon is at the origin of many applications, for example in sensing [6–10], in design of metamaterials [11], for single molecule detection [12,13], and in spectroscopic techniques [14]. In general, coupling and optical properties of samples strongly depend on the distance between nanoparticles [15,16]. In particular, in a gold nanoparticle dimer, once the gap between the two particles is as small as half of their diameter or less, the coupling leads to a shift of the plasmon resonance peak [17], which exponentially depends on the gap value [18,19]. Thus, interesting opportunities would emerge from the possibility to dynamically control the distance between the coupled plasmonic particles of a macroscopic sample at the nanometer scale [20–23]. In the following, we show that realization of this control can be as simple as pulling an

*Address correspondence to Roberto Caputo, Department of Physics, Centre of Excellence for the Study of Innovative Functional Materials CEMIF-CAL, University of Calabria and CNR-IPCF–LICRYL 87036, Arcavacata di Rende, Italy. E-mail: roberto.caputo@fis.unical.it

Color versions of one or more of the figures in the article can be found online at www.tandfonline.com/gmcl.

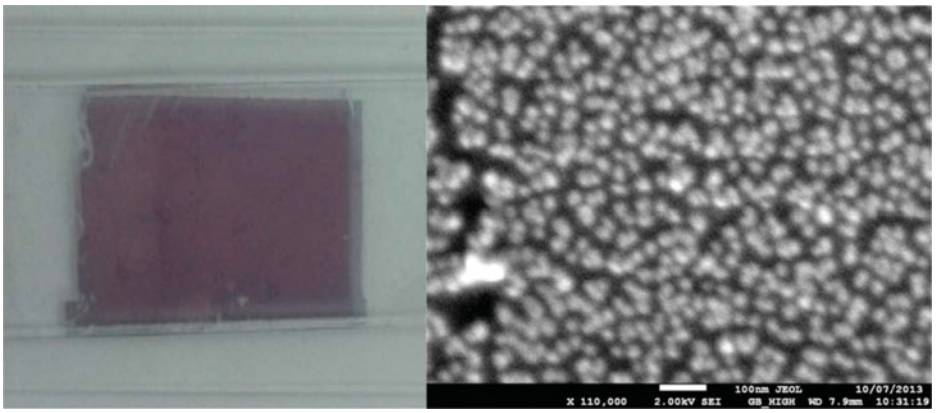

Figure 1. (a) Photograph of the PDMS tape covered with gold nanoparticles that have undergone a growth procedure; (b) SEM micrograph of the same sample.

elastic tape covered by gold nanoparticles: The distance between nanoparticles is, indeed, mechanically modified by stretching the elastic tape in one direction, an effect that results is a macroscopic colour change of the sample. At the nanoscale, this means that the electric field in the gap between the particles can be manipulated by using a mechanical strain.

Sample Design and Fabrication

A tape covered with gold-nanoparticles has been realized by first functionalizing a flexible polydimethylsiloxane (PDMS) substrate, so that gold nanoparticles spontaneously adsorb and are immobilized onto its surface in a charge-driven process. The resulting surface reveals an amorphous arrangement of well-separated non-interacting particles. The sample prepared this way underwent then a chemical procedure for growing the gold nanoparticles in size, directly in their site. Details on the sample preparation can be found in ref. [24]. On the surface of the red colored sample shown in Fig. 1a, grown nanoparticles have an average diameter of about 32 nm (Fig. 1b) and a center-to-center average distance of about 39 nm. Once the sample has been prepared, a simple mechanical stretching (of a few percent) is applied to the tape, which induces plasmonic coupling between neighbor nanoparticles.

As depicted in Fig. 2a, stretching of the tape in one direction leads to compression in the orthogonal one. In literature, other techniques are reported to obtain plasmon tuneability and/or coupling between nanoparticles of fixed size, coated on, or embedded in, flexible substrates [20,25–28]. In our case, the fine increase of the particle size is a necessary condition to obtain coupling: the growth procedure gradually reduces the inter-particle gap up to the trigger of the plasmon coupling (Fig. 2b), whereas application of a mechanical stretching is sufficient to allow its reversible tuning. In Fig. 2c, pictures of the sample are reported, which show different colors, before (on the left) and after the stretching (on the right), respectively.

Spectroscopic Characterization and Results

First of all, we have verified that, during the applied stretching, the PDMS substrate is still in an elastic regime (Poisson ratio of about 0.5) [29]. This has been done by taking, at each stretching state, a picture of the sample; pictures have then been analyzed (by using the

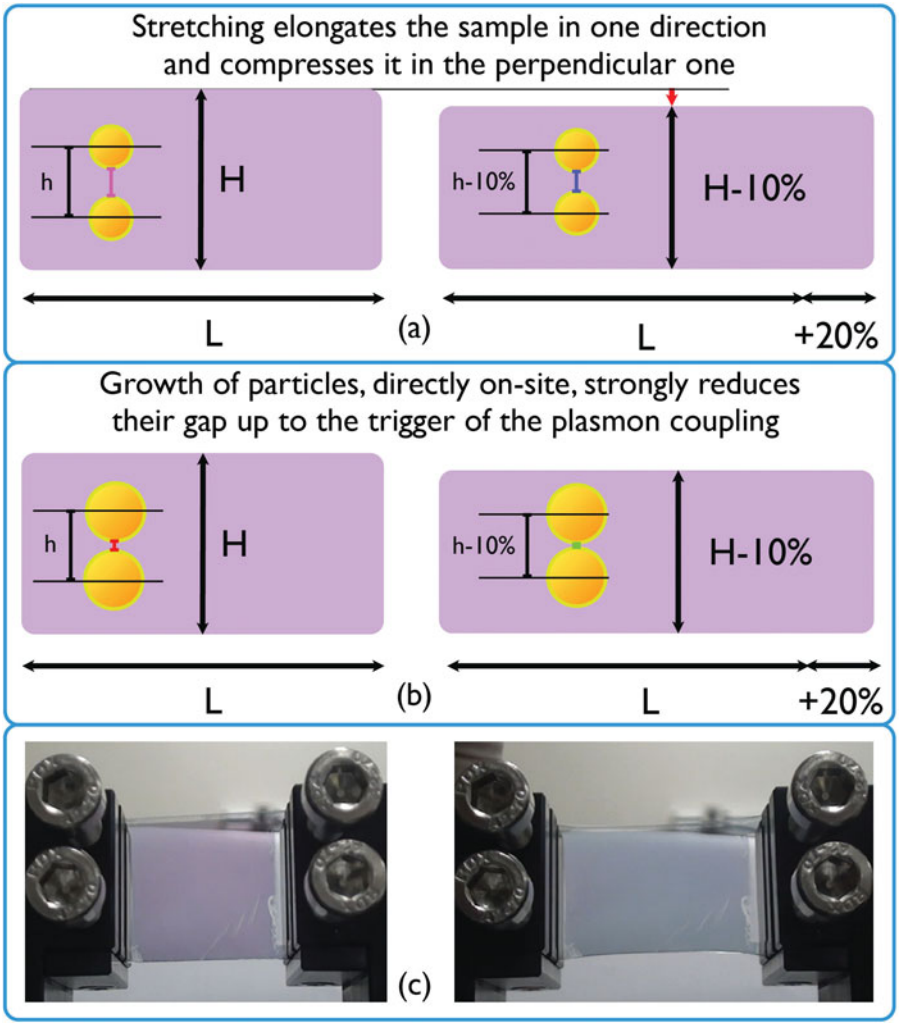

Figure 2. (a) Sketch of the PDMS tape covered with gold nanoparticles. By stretching the tape, the average distance between nanoparticles becomes larger in the stretching direction and shorter in the perpendicular one; (b) the growth procedure gradually reduces the inter-particle gap up to the trigger of the plasmon coupling; stretching of the sample is accompanied by a remarkable change of color, from purple-red (c, on the left) to blue-violet (c, on the right). Images were acquired with a polarizer, mounted onto a camera, with polarization direction perpendicular to the applied strain direction.

"ImageJ" software) with the aim of measuring the actual length and width of the sample. Obtained values have been used to calculate the percentage of compression the sample underwent in the direction perpendicular to the applied strain. Within the experimental error, all obtained values confirm a Poisson ratio of about 0.5 (0,4996 $\pm$ 0,0283), up to a 20.8% of stretching (Fig. 3a); this confirms that the sample is in the elastic regime for all the applied strains.

As for spectroscopic characteristics, quite surprisingly, our samples, which are amorphous and initially isotropic, develop highly polarization-dependent optical properties after

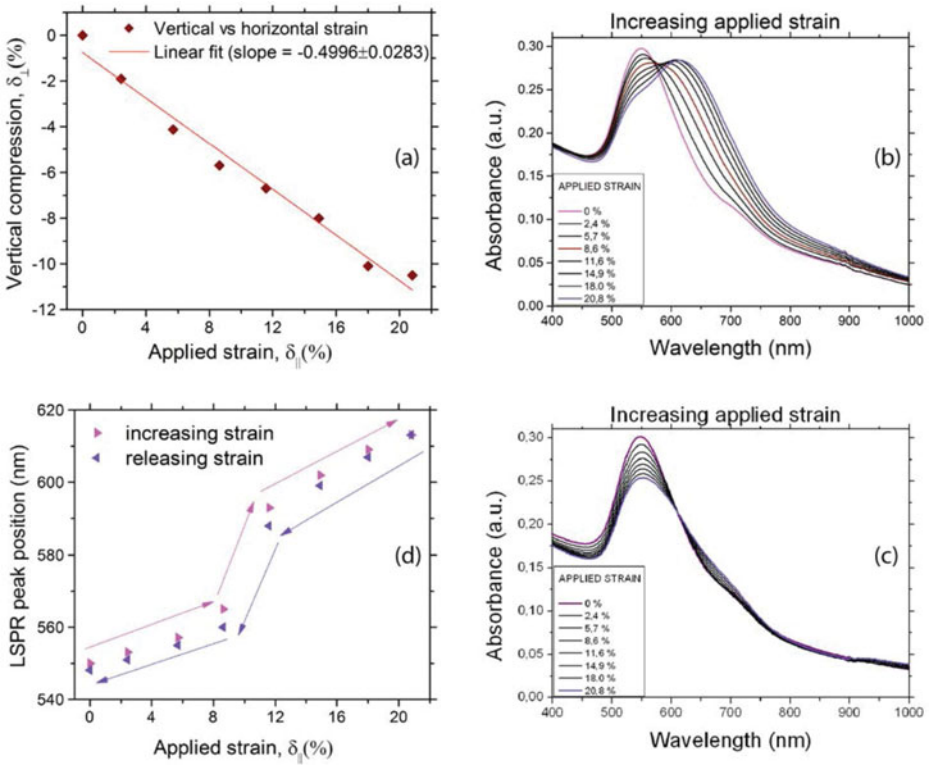

Figure 3. Measurement of the compression the sample undergoes in the direction perpendicular to the applied strain. A Poisson ratio of about 0.5 is confirmed for the PDMS substrate (a). Extinction spectra of the sample coated with gold nanoparticles (after twelve cycles of growth) acquired while increasing the applied strain from 0% to 20.8%; the sample has been irradiated with (b) light polarized perpendicularly to the stretching direction, and (c) light polarized parallel to the stretching direction. Spectral position of the resonance peak maxima as a function of the applied strain (d) during a straining-releasing cycle. A slight hysteresis is observed.

undergoing a stretching of about 20% only. Indeed, the macroscopic color change of the sample is accompanied by a polarization dependent variation of the extinction spectra (Fig. 3b,c). In fact, while a pronounced red-shift of the plasmon resonance is observed with an exciting light linearly polarized in the direction perpendicular to the stretching, no shift is observed when the light polarization direction is parallel to the stretching direction. In addition, it is worth noting that the plasmonic red-shift resulting from the mechanical action is perfectly reversible and indefinitely reproducible. Fig. 3d shows the variation of the spectral position of the resonance peak maxima as a function of the strain during a straining-releasing cycle. The presence of a slight hysteresis assures a fairly good reversibility of the shift. The plasmonic shift, obtained upon stretching of the sample (Fig. 3b), is quite remarkable and we have investigated the theoretical scenario behind this effect by considering in first approximation, for non-touching particles, the interaction energy of a dimer. The impinging polarized light induces a dipole in each nanoparticle; the dimer can be, therefore, represented by two dipoles, initially separated by the vectorial distance $\boldsymbol{r}$ (center-to-center), which forms an angle α with the stretching direction (x). In this way, the coupling between nanoparticles can be described by using the exciton-coupling model

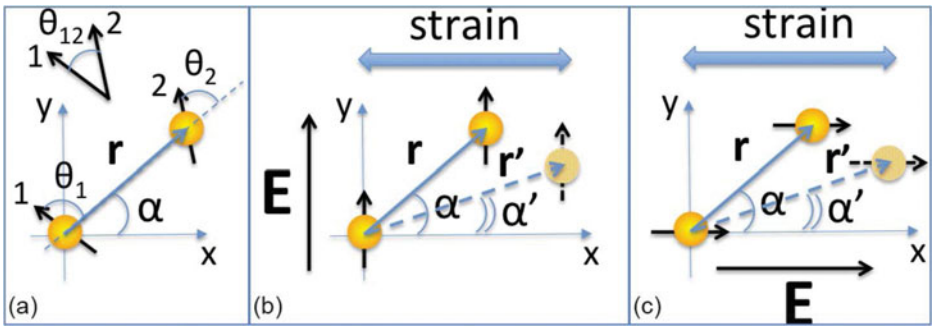

Figure 4. Sketch of coupled nanoparticles considered as interacting dipoles; (a) generic geometry of two interacting dipoles; (b) Excitation of a dimer with perpendicularly polarized light and geometrical configuration with and without applied strain; (c) Excitation of a dimer with parallel polarized light and geometrical configuration with and without applied strain.

[30], originally developed to explain shifts observed in the spectra of dimerized organic molecules. In this framework, the interaction energy U between the two dipoles of a dimer can be written as

$$U = -\frac{\xi |\mu|^2}{4\pi \varepsilon_0 r^3} \tag{1}$$

where μ is the dipole moment of each particle of the dimer and the factor $\xi = 3cos\theta_1 cos\theta_2 - cos\theta_{12}$ takes into account the relative orientation of the interacting dipoles between each other and with respect to the exciting field $\boldsymbol{E}$, as sketched in Fig. 4a.

In more detail, θ_1 and θ_2 are the angles formed by dipole 1 and dipole 2 with $\boldsymbol{r}$ respectively, while θ_{12} is the angle they form with each other. If the relative position of the two interacting dipoles is modified by the strain applied to the PDMS substrate they are immobilized wherein, the energy variation ΔU related to the new configuration can be written as:

$$\Delta U = U'_{\perp,//} - U_{\perp,//} = -\left(\frac{\xi'_{\perp,//} |\mu|^2}{4\pi \varepsilon_0 r'^3} - \frac{\xi_{\perp,//} |\mu|^2}{4\pi \varepsilon_0 r^3} \right) \tag{2}$$

where $r' = r[(1+\delta)^2 ... (1-0.5\delta)^2 sin^2\alpha]^{1/2}$ is the distance, after strain, between the considered particles and α is the initial angle made by $\boldsymbol{r}$ with the x-axis (Fig. 4b,c). In the expression for r', it has been also considered that, for all applied strains ($\delta = 0\% \div 20.8\%$), the PDMS sample is in the elastic regime (PDMS Poisson's ratio ≈ 0.5). As far as ξ values are considered, since dipoles 1 and 2 are induced by the exciting field $\boldsymbol{E}$, they are oriented parallel to it, hence $\theta_1 = \theta_2 = \theta_{\perp,\parallel}$ and $\theta_{12} = 0$, while $\theta_\perp = \pi/2 - \alpha$ for light polarized perpendicularly to the strain ($\boldsymbol{E} \perp \boldsymbol{x}$) and $\theta_{//} = \alpha$ for light polarized parallel to the strain ($\boldsymbol{E}//\boldsymbol{x}$). Thus, in our specific case, the polarization-dependent expressions for ξ are:

$$\xi_\perp = 3\cos^2(\pi/2 - \alpha) - 1;\ \xi// = 3\cos^2(\alpha) - 1 \tag{3}$$

In Fig. 5a,b, Eq. 2 is plotted as a function of the angle α and for several different values of the strain parameter δ. For a given polarization of the exciting light, the energy variation strongly depends on the angular interval that α belongs to. In particular, Fig. 5a indicates that, if the light field $\boldsymbol{E}$ is perpendicular to the stretching direction, $\Delta U_\perp < 0$ for

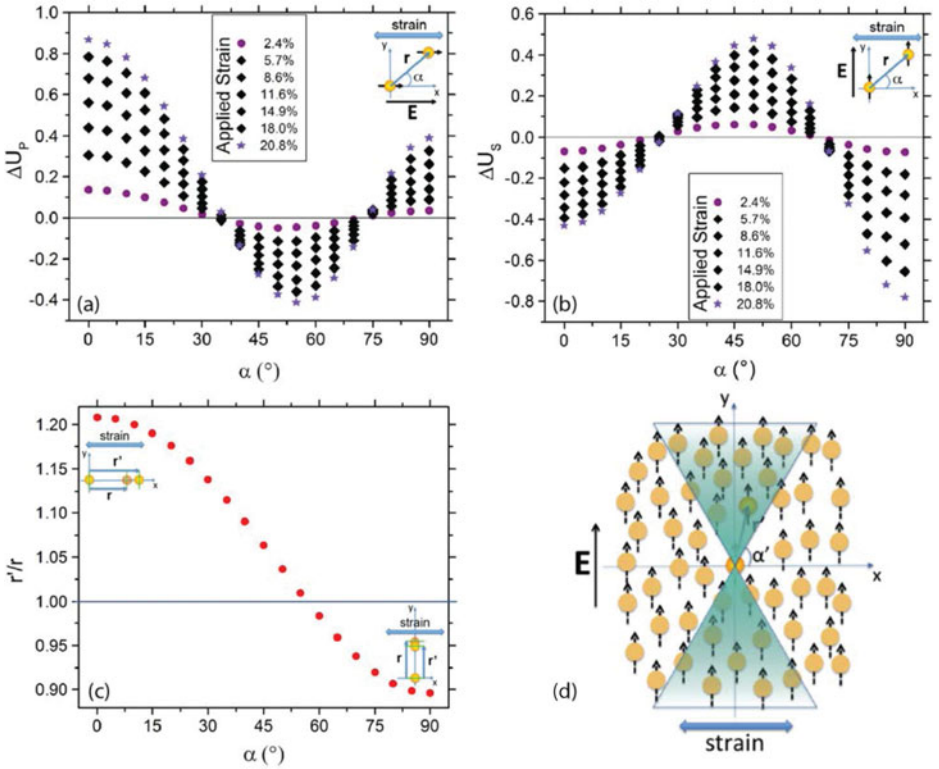

Figure 5. Stretched-unstretched interaction energy variation (referred to the initial value of the interaction energy) plotted as a function of the angle made by the inter-dipole axis with the x-axis both for (a) s- and (b) p-polarized exciting light. Note that this is true for all initial distances *r*. (c) Plot of the ratio between the inter-particle distance (center-to-center) before (*r*), and after (*r*') stretching. The upper left and lower right insets show the condition of two gold nanoparticles that, upon stretching, undergo an increase and a decrease of their inter-particle distance respectively; (d) A dipole and its neighbors are considered. Upon stretching, and starting from an uncoupled condition, this dipole potentially only interacts with the ones laying in a well-defined double angular cone with an aperture of 60° because only for the dipoles in this angular region the distance decreases upon stretching (r'/r<1).

$0° < \alpha < 25°$ and $70° < \alpha < 90°$, while $\Delta U_{\perp} > 0$ for $25° < \alpha < 70°$. For $\Delta U_{\perp} < 0$ ($\Delta U_{\perp} > 0$) a red-shift (blue-shift) of the plasmon band is expected. Since in the relaxed state the particles are (almost) non interacting, above considerations on $\Delta U_{\perp}$ and related shifts can apply only to those dimers whose inter-distance r decreases upon stretching. As shown in Fig. 5c, this holds only for large angles ($60° < \alpha < 90°$). In other words, only a limited number of dipoles undergo plasmon coupling during the stretching experiment. When considering a given dipole and its nearest neighbors, this dipole potentially interacts only with the ones lying in a well-defined double angular cone with an aperture of 60° (Fig. 5d). Due to the effect of the angle α both on distance and interaction energy, a pronounced dependence of the plasmon shift on the polarization of the impinging light is, in fact, expected. In case of an exciting light whose electric field is polarized parallel to the stretching direction, the situation is reversed.

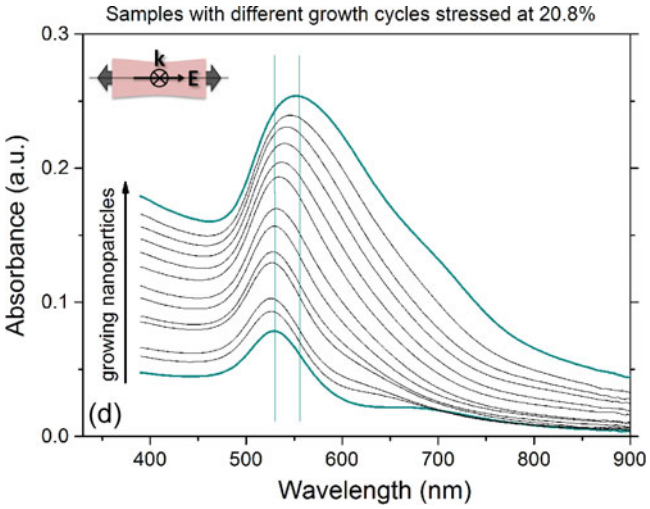

Figure 6. Extinction spectra of the gold nanoparticle coated PDMS samples undergoing different cycles of growth of the particles with an applied strain of 20.8%. Samples have been excited with a p-polarized light.

In this case, indeed, for small and large α angles ($0^\circ < \alpha < 35^\circ$ and $75^\circ < \alpha < 90^\circ$), the applied strain yields a blue-shift of the plasmon while, for intermediate angles ($35^\circ < \alpha < 75^\circ$), a red-shift is expected. Again, we only consider the interval $60^\circ < \alpha < 90^\circ$, since only in this case r decreases upon stretching. In this angular region, Fig. 5b indicates that red- and blue-shift are comparable. This conclusion is experimentally verified in Fig. 6, where the overall plasmonic red-shift is very limited for the sample excited with parallel polarized light and the main result is a mere broadening of the plasmon band.

Above considerations explain the strong polarization dependent behavior of the amorphous and initially isotropic samples when stretched by about 20% or even less. Key to this behavior is the growth of the particle size, such that the gap s between them (more precisely s/D) enables a weak coupling. In order to quantitatively demonstrate how the combined effect of nanoparticle growth and stretching influence the average normalized gap between particles, we have analyzed the behavior of scaled gap (s/D) and red-shift ($\Delta\lambda/\lambda_0$) from the 7th to the 12th cycle of growth, at rest and at maximum stretching. The two graphs, reported in Fig. 7a,b, resume this analisys and show the fundamental contribute of the mechanical strain to develop a strong plasmonic coupling. In the graph reported in Fig. 7a, a constant and noticeable decrease of the relative gap of 59% is observed for every cycle of growth here considered. In Fig. 7b, by increasing the number of growth cycles, two different behaviors of the scaled plasmonic red-shift appear, in case of sample at rest and under maximum stretching. In the former, the red-shift increases almost linearly while in the latter (sample at maximum stretching), it undergoes a nonlinear variation and, at the 12^{th} cycle of growth, the scaled red-shift increases from 0.0397 to 0.15, corresponding to a significant variation of about 280% (Fig. 7b).

By comparing the two graphs it is possible to relate the decrease of the average interdistance between the randomly distributed nanostructures (induced by the application of a mechanical strain to the elastomeric tape covered by grown gold nanoparticles) to the increase of the plasmonic shift. Indeed, it is reported in literature that a plot of the scaled

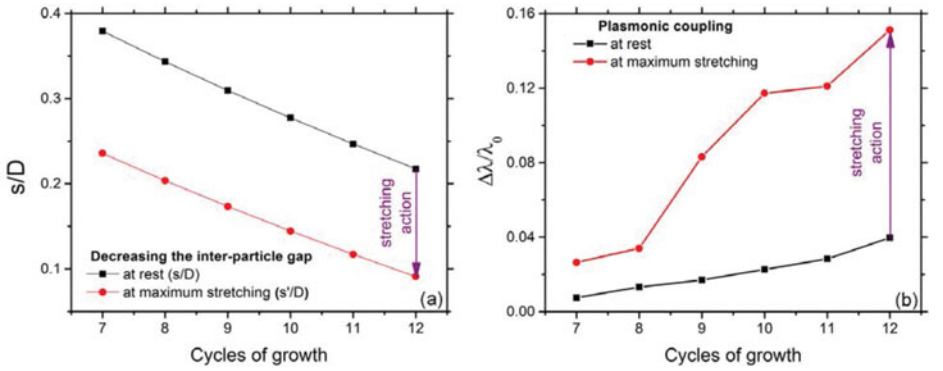

Figure 7. (a) Effect of stretching on the inter-particle gap normalized to the particle diameter and (b) plasmonic shift normalized to the single particle plasmonic response.

shift in terms of the scaled gap has shown an exponential trend, but only for systems made of periodic arrays of nanoparticles, as already observed by El-Sayed [18].

Conclusions

In conclusion, we have realized a macroscopic strain-dependent optical pad based on a bottom-up, self-assembly principle. Upon slight stretching, the amorphous and initially isotropic sample reversibly develops a strong polarization-dependent variation of its optical properties, which is accompanied by a macroscopic change of color. This effect is due to nanoscale variations in inter-particle separations, which have dramatic effects on the plamonic coupling strength between particles. The possibility of continuously tuning this coupling by applying a macroscopic mechanical solicitation represents the key feature of this novel platform: its exploitation can enable a detailed study of the plasmonic coupling effect, with an unprecedented sensitivity as well as the realization of advanced applications in sensing and strain detectors.

Acknowledgments

The authors would like to acknowledge the contribution of the COST Action IC1208. www.ic1208.com. Financial support from the University of Geneva is kindly acknowledged.

References

[1] Kreibig, U., & Vollmer, M. (1995) *Optical properties of metal clusters*. Springer.
[2] Mie, G. (1908) Articles on the optical characteristics of turbid tubes, especially colloidal metal solutions. *Ann. Phys.*, *25*, 377–445.
[3] Maier, S. A. (2007) Plasmonics: Fundamentals and Applications. Springer.
[4] Halas, N. J., Lal, S., Chang, W. S., Link, S., & Nordlander, P. (2011) Plasmons in Strongly Coupled Metallic Nanostructures. *Chem. Rev.*, *111*, 3913–3961.
[5] Su, K. H. *et al.* (2003) Interparticle coupling effects on plasmon resonances of nanogold particles. *Nano Lett.*, *3*, 1087–1090.
[6] Willets, K. A., & Van Duyne, R. P. (2007) in *Ann. Rev. of Phys. Chem. Annual Review of Physical Chemistry*, Vol.. *58*, 267–297.

[7] Haes, A. J., Zou, S. L., Schatz, G. C., & Van Duyne, R. P. (2004) A nanoscale optical biosensor: The long range distance dependence of the localized surface plasmon resonance of noble metal nanoparticles. *J. Phys. Chem. B* , *108*, 109–116.
[8] Li, J. F. *et al.* (2010) Shell-isolated nanoparticle-enhanced Raman spectroscopy. *Nature*, *464*, 392–395.
[9] Liu, N., Tang, M. L., Hentschel, M., Giessen, H., & Alivisatos, A. P. (2011) Nanoantenna-enhanced gas sensing in a single tailored nanofocus. *Nature Mater.*, *10*, 631–636.
[10] Schuller, J. A. *et al.* (2010) Plasmonics for extreme light concentration and manipulation. *Nature Mater.*, *9*, 193–204.
[11] Rockstuhl, C., Lederer, F., Etrich, C., Pertsch, T., & Scharf, T. (2007) Design of an artificial three-dimensional composite metamaterial with magnetic resonances in the visible range of the electromagnetic spectrum. *Phys. Rev. Lett.*, *99*, 017401.
[12] Bailo, E., & Deckert, V. (2008) Tip-enhanced Raman scattering. *Chem. Soc. Rev.*, *37*, 921–930.
[13] Ghosh, S. K., & Pal, T. (2007) Interparticle coupling effect on the surface plasmon resonance of gold nanoparticles: From theory to applications. *Chem. Rev.*, *107*, 4797–4862.
[14] Mayer, K. M., & Hafner, J. H. (2011) Localized Surface Plasmon Resonance Sensors. *Chem. Rev.*, *111*, 3828–3857.
[15] Kinnan, M. K., & Chumanov, G. (2010) Plasmon coupling in two-dimensional arrays of silver nanoparticles: II. effect of the particle size and interparticle distance. *J. Phys. Chem. C*, *114*, 7496–7501.
[16] Cunningham, A., Muhlig, S., Rockstuhl, C., & Burgi, T. (2011) Coupling of plasmon resonances in tunable layered arrays of gold nanoparticles. *J. Phys. Chem. C*, *115*, 8955–8960.
[17] Jain, P. K., & El-Sayed, M. A. (2010) Plasmonic coupling in noble metal nanostructures. *Chem. Phys. Lett.*, *487*, 153–164.
[18] Jain, P. K., Huang, W. Y., & El-Sayed, M. A. (2007) On the universal scaling behavior of the distance decay of plasmon coupling in metal nanoparticle pairs: A plasmon ruler equation. *Nano Lett.*, *7*, 2080–2088.
[19] Sonnichsen, C., Reinhard, B. M., Liphardt, J., & Alivisatos, A. P. (2005) A molecular ruler based on plasmon coupling of single gold and silver nanoparticles. *Nature Biotech.*, *23*, 741–745.
[20] Millyard, M. G. *et al.* (2012) Stretch-induced plasmonic anisotropy of self-assembled gold nanoparticle mats. *Applied Physics Letters*, *100*.
[21] Zhu, X. L., Shi, L., Liu, X. H., Zi, J., & Wang, Z. L. (2010) A Mechanically Tunable Plasmonic Structure Composed of a Monolayer Array of Metal-Capped Colloidal Spheres on an Elastomeric Substrate. *Nano Research*, *3*, 807–812.
[22] Zhu, X. L. *et al.* (2012) A stretch-tunable plasmonic structure with a polarization-dependent response. *Optics Express*, *20*, 5237–5242.
[23] Chiang, Y. L. *et al.* (2010) Mechanically tunable surface plasmon resonance based on gold nanoparticles and elastic membrane polydimethylsiloxane composite. *Applied Physics Letters*, *96*.
[24] Cataldi, U., Caputo, R., Kurylyak, Y., Klein, G., Chekini, M., Umeton, C., Bürgi, T., (2014) Growing gold nanoparticles on a flexible substrate to enable simple mechanical control of their plasmonic coupling. *J. Mat. Chem. C*, *2*, 7927–7933.
[25] Malynych, S., & Chumanov, G. (2003) Light-induced coherent interactions between silver nanoparticles in two-dimensional arrays. *J. Am. Chem. Soc.*, *125*, 2896–2898.
[26] Zhu, X. L., Shi, L., Liu, X. H., Zi, J., & Wang, Z. L. (2010) A Mechanically Tunable Plasmonic Structure Composed of a Monolayer Array of Metal-Capped Colloidal Spheres on an Elastomeric Substrate. *Nano Res.*, *3*, 807–812.
[27] Chiang, Y. L. *et al.* (2010) Mechanically tunable surface plasmon resonance based on gold nanoparticles and elastic membrane polydimethylsiloxane composite. *Appl. Phys. Lett.*, *96*.

[28] Zhu, X. L. *et al.* (2012) A stretch-tunable plasmonic structure with a polarization-dependent response. *Opt. Exp.*, *20*, 5237–5242.
[29] Pritchard, R. H., Lava, P., Debruyne, D., & Terentjev, E. M. (2013) Precise determination of the Poisson ratio in soft materials with 2D digital image correlation. *Soft Matter*, *9*, 6037–6045.
[30] Kasha, M. (1963) Energy transfer mechanisms and molecular exciton model for molecular aggregates. *Radiation Res.*, *20*, 55-&.